Materials Research. 2014; 17(4): 947-957
DOI: http://dx.doi.org/10.1590/S1516-14392014005000096
© 2014

Electrodeposition of Cobalt Rich Zn-Co alloy Coatings from Citrate Bath

Julyana Ribeiro Garcia, Dalva Cristina Baptista do Lago, Lilian Ferreira de Senna*

Corrosion and Electrochemistry Laboratory – LEC, Chemistry Institute, Rio de Janeiro State University – UERJ, Rua São Francisco Xavier, 524, Pavilhão Haroldo Lisboa da Cunha, S. 427, Maracanã, CEP 20550-013, Rio de Janeiro, RJ, Brazil

Received: December 11, 2013; Revised: April 17, 2014

Zn-Co alloy coatings were produced on carbon steel, at room temperature, from citrate baths (0.100 mol L^{-1}) containing $[Zn^{2+}] = [Co^{2+}] = 0.05$ mol L^{-1}. Coatings with **%m/m Co > %m/m Zn** were observed under all deposition conditions, except for **I** = 10 A m^{-2}. As the current density (**I**) was increased, a significant decrease ($p<0.05$) in **%m/m Zn** was noted, and the highest value of **% m/m Co** was observed at 80 A m^{-2}. The Co-rich coatings presented refined microstructure, with small grain sizes. The smallest $\mathbf{I}_{corr}$ of the studied substrate/coatings systems, 2.4 μA cm^{-2}, was obtained at **I** = 10 A m^{-2}. Under these conditions, the coatings contained ~ 30 % m/m Co and 70 % m/m Zn and only the γ-ZnCo phase was obtained. The $\mathbf{I}_{corr}$ found in the present work is smaller than those usually found in the literature for Zn-Co coatings with small Co content.

Keywords: *Electrodeposition, Zn-Co alloy coatings, sodium citrate, corrosion protection*

1. Introduction

Zn coatings are generally used to protect steel components, acting as sacrifice coatings, and decreasing the substrate material corrosion[1]. Szczygiel et al.[2] and Chen and Sun[3] have shown that the co-deposition of zinc with other metals, such as nickel, iron and cobalt, enhances the anticorrosive properties of the zinc coatings. Additionally, the use of these metals to produce Zn-alloy coatings may be an ecological alternative to the high toxicity of Zn-Cd coatings[4].

The electrodeposition processes of Zn-Ni, Zn-Fe, and Zn-Co alloys are considered anomalous, that is, the deposition of less noble metal ion Zn (II) is favored when compared to the other alloy metal ions[5]. This anomalous process is reported by many works in the literature[4,6-9] and various explanations of the anomaly have been suggested, e.g. underpotential codeposition (UPD), kinetic behavior, the hydroxide suppression mechanism, and the influence of Co (III)[10]. However, it is always considered that certain experimental conditions, such as high values of current density (I), for example, can change the process from anomalous to normal and under these conditions the Zn-Co alloy coatings presented a cobalt content higher than that of zinc[11,12].

The increase in cobalt content in the Zn-Co coating can be interesting for the anticorrosive performance of these layers. Kirilova et al.[12] have observed that coatings containing small cobalt content could still be considered as sacrifice coatings, while those with high amount of this metal were nobler than steel, acting as anticorrosive barrier. In addition, Lichušina et al.[10] have showed that Co-rich Zn-Co coatings (15-18 % m/m Co) presented good appearance and high corrosion resistance in NaCl solution. Lima-Neto et al.[13] have shown similar results for a Zn-Co alloy coating with 18 % m/m Co. However, there is no consensus in the literature concerning this topic. In most of the works, the anticorrosive performance of the alloy decreased with the elevation in **% m/m Co**[8,14].

Generally, to fulfill the coatings requests for a better performance, the metallic-alloy deposition baths are always developed and/or modified to enhance the cathodic current efficiency, the amount of certain metal in the coating, or even to refine the grain sizes and the decorative characteristics of the coatings[8,12]. For this purpose, a complexant agent or a leveling additive can be added to an electrodeposition bath, causing several changes on the reduction mechanism of the ions in the solution and/or in the activation energy of the electrode surface[15-17]. For this reason, it is possible to find several works concerning the production of Zn-Co coatings from acidic or alkaline baths, containing additives and/or complexant agents[7,8,10,18]. Despite its well known toxicity and the rigorous maintenance control to avoid environmental problems[19,20], the traditional cyanide-containing alkaline baths are sometimes used for electroplating of Zn and Zn alloys. Following the general trends for the electrodeposition of alloy coatings, however, most of the current researches found in the literature deals with nontoxic or environmentally friend complexant agents and additives[2,7,8,21-24].

Earlier, we have used a nontoxic citrate bath to produce Cu-Zn and Cu-Co alloy coatings on steel substrate[25,26]. In both cases, protective coatings with high anticorrosive performance were obtained, depending on the deposition parameters used. The quality of these coatings was considered satisfactory, even at high values of current density. Therefore, based on these results, the present work aims to study the production of Co-rich Zn-Co alloy coatings

*e-mail: lsenna@uerj.br

Table 1. Chemical composition and pH values of the studied solutions.

Solution	Composition/mol L^{-1}			pH
	$CoSO_4.6H_2O$	$ZnSO_4.5H_2O$	$Na_3C_5H_6O_7$	
1	0.05	-	-	4.85
2	-	0.05	-	6.12
3	0.05	-	0.10	6.50
4	-	0.05	0.10	6.45
5	0.05	0.05	0.10	6.23

on a carbon steel substrate, from a citrate-base bath. Our goals are to verify the influence of citrate in the bath for Zn-Co deposition and evaluate the effects of current density (**I**) on the cathodic current efficiency ($\mathbf{E}_f$), the metal contents in the coatings (**% m/m Zn** and **% m/m Co**), and on the coatings' morphology, texture and corrosion performance. This way, we intend to contribute to a better understanding about the Zn-Co reduction from this kind of bath, producing Co-rich coatings with a higher anticorrosive performance.

2. Experimental Procedures

2.1. *Voltammetric experiments*

The voltammetric experiments were carried out in the electrolyte solutions described in Table 1.

It was used a three-electrode cell consisted of graphite as the working electrode (exposed area = 0.28 cm^2), a Pt spiral as the counter electrode, and the reference electrode was a saturated mercury (I) sulfate electrode (Hg/Hg_2SO_4), SSE. The working electrode was always polished with emery paper (600 mesh), washed with deionized water and alcohol and finally dried, before being immersed in each experiment. The Pt spiral was immersed in 20 %v/v HNO_3 solution for 1 minute, immediately before being used in the experiments, to remove any oxide layer that could be present. The voltammetric experiments were performed without stirring in a potentiostat/galvanostat *AUTOLAB PGSTAT 302 N* from 0 to –1.6 V_{SSE}, with a scanning rate of 1 mV s^{-1}.

2.2. *Cathodic polarization curves*

Cathodic polarization curves of the steel substrate were galvanostatically obtained in the solution 5 of Table 1, in the current density range from 0.1 to 120 A m^{-2} using a potentiostat/galvanostat developed for this purpose[25,26]. AISI 1020 carbon steel discs (area = 4.90 x 10^{-4} m^2) were used as working electrodes. These samples were first polished with emery paper (100 to 600 mesh), washed with deionized water and alcohol and finally dried, before being immersed in the solutions. The counter electrode was platinum net, which was cleaned in a similar way earlier described for the voltammetric experiments. The reference electrode was the same saturated mercury (I) sulfate electrode (Hg/Hg_2SO_4), SSE. The experiments were carried out at room temperature with a stirring speed of 300 rpm.

2.3. *Electrodeposition experiments*

The electrodeposition experiments were carried out in triplicate series, using the same potentiostat/galvanostat and the electrochemical cell earlier described in topic 2.2, as well as the same cleaning procedures for both the work and the counter electrodes used. Based on the polarization curves, four values of **I** (10 A m^{-2}, 20 A m^{-2}, 40 A m^{-2} and 80 A m^{-2}) were selected to produce the Co-rich Zn-Co alloys on a steel substrate from the Bath 5 of Table 1 at the same stirring speed (300 rpm). Each electrodeposition time was calculated, based on the Faraday's law, to produce a 10 mg coating. The conditions for the electrodeposition experiments are shown in Table 2.

Table 2. Experimental conditions to produce Zn-Co coatings from citrate bath.

Experiment no.	$[Co^{2+}]$ / mol L^{-1}	I / A m^{-2}
1	0.05	10
2	0.05	20
3	0.05	40
4	0.05	80

The produced layers were dissolved in 20 %v/v HNO_3, and the alloy composition was determined by flame atomic absorption spectrometry (FAAS), applying the conditions recommended by the instrument operation manual (*AANALYST 300*). These results and the theoretical mass obtained from Faraday's law were used to calculate the $\mathbf{E}_f$ value for each deposition time[18,25,26].

The content of each metal in the coatings was calculated as the **% m/m Co** and **% m/m Zn**, using Equations 1 and 2, respectively.

$$\%m / mCo = \frac{m_{Co}}{m_{Co} + m_{Zn}} \times 100\% \quad (1)$$

$$\%m / mZn = \frac{m_{Zn}}{m_{Co} + m_{Zn}} \times 100\% \quad (2)$$

The cobalt content in the electrodeposition bath (Bath 5 of Table 1) was also calculated using Equation 1. The metallic contents of the electrodeposited coatings were compared with these results.

Based on the electrodeposition experiments, partial polarization curves were obtained by calculating the effective currents densities used for zinc and cobalt deposition ($\mathbf{I}_{Co}$ and $\mathbf{I}_{Zn}$, respectively) from the element contents in the alloy coating and the current efficiency. In each case, the partial currents were associated with the corresponding potential response of the total applied current density. The effective

currents densities for hydrogen ($\mathbf{I}_H$) were obtained by decreasing the applied **I** from the summation of $\mathbf{I}_{Co}$ and $\mathbf{I}_{Zn}$.

2.4. *Morphological analysis*

Scanning electron microscopy (SEM) was performed using a *ZEISS EVO MA-10* microscope to evaluate the effect of the deposition parameters on the surface morphology of the coatings. The samples were cleaned with alcohol, dried and adapted to the stub with a conductive tape. The analyses were carried out in high vacuum and in the secondary electron mode. An X-rays energy dispersive spectrometer, EDS (*EDS IFRX*), coupled to the microscope, was used for elemental mapping at selected regions of the sample.

2.5. *Microstructure characterization*

X-rays diffractograms (XRD) of the coatings were obtained using a diffractometer (R*igaku Miniflex II*) with a copper source (CuK = 1.5406 Å), at 40 kV. The 2θ ranged from 10° to 120°, at a scanning rate of 0.050° s^{-1}. The more prominent diffractogram lines from the Zn-Co alloy deposit were fitted by a Gaussian equation (using Microcal Origin®, release 8.0) to obtain their 2θ values, which used to calculate the *d* (h k l) parameters of the diffraction lines.

2.6. *Corrosion experiments*

Zn-Co coatings were produced on steel substrate at chosen conditions, based on the chemical, microstructural, and morphological results earlier obtained. Polarization curves were performed in these selected coating/substrate systems employing a potentiostat/galvanostat *AUTOLAB PGSTAT 302N*. The working electrode (that is, each coating/substrate system produced) was immersed in a 0.5 mol L^{-1} NaCl solution (pH = 7.06) and a linear voltametry was carried out from –2 V_{SCE} to 1 V_{SCE}, with a scanning rate of 1 mV s^{-1}, at room temperature. The counter electrode was a platinum net, while the reference electrode was a saturated calomel electrode (SCE). The corrosion current density values ($\mathbf{I}_{corr}$) and the corrosion potential ($\mathbf{E}_{corr}$) were obtained by Tafel extrapolation.

3. Results and Discussion

3.1. *Cathodic linear voltametric curves*

The voltametric experiments aimed to study the effect of the citrate ligand on the deposition process of zinc and cobalt ions. Citrate is present in the baths as a ligand, which may influence on the alloy deposition process. Additionally, the differences among the deposition processes of the Zn-Co alloy from a citrate bath and those from the separated metals ions in similar baths were also evaluated.

Figure 1 shows the differences in the cathodic scans among the solutions containing one of the ions (Co (II) or Zn (II)), with or without citrate. During the scans towards negative potentials, the cathodic current of the processes obtained in baths without citrate (Solutions 1 and 2 of Table 1) increased sharply once cobalt or zinc nucleation began (Figure 1a). For Solution 1, containing only Co (II), the cathodic current density reached a maximum value at approximately –1.211 V. The peak formation was then followed by a slow decay to a steady state. This behavior corresponds to a diffusion controlled process. On the other hand, the deposition peak was not very well resolved for Solution 2 (containing only Zn (II)), which suggests the existence of other processes in addition to mass control. The analysis of the isolated curves shows that the deposition of cobalt starts at more positive potentials, confirming that Co (II) behaves as the noblest ion.

The stability constants for Zn-Citrate complex and Co-citrate complex[27] are, respectively, $K_f^{Zn} = 4.45 \times 10^7$ and $K_f^{Co} = 6.76 \times 10^4$, suggesting that the reduction of both metallic ions would be more difficult in a bath containing sodium citrate. However, the potential where a significant variation in the cathodic current density was noted (which was considered the starting deposition potential, E_{sd}), was

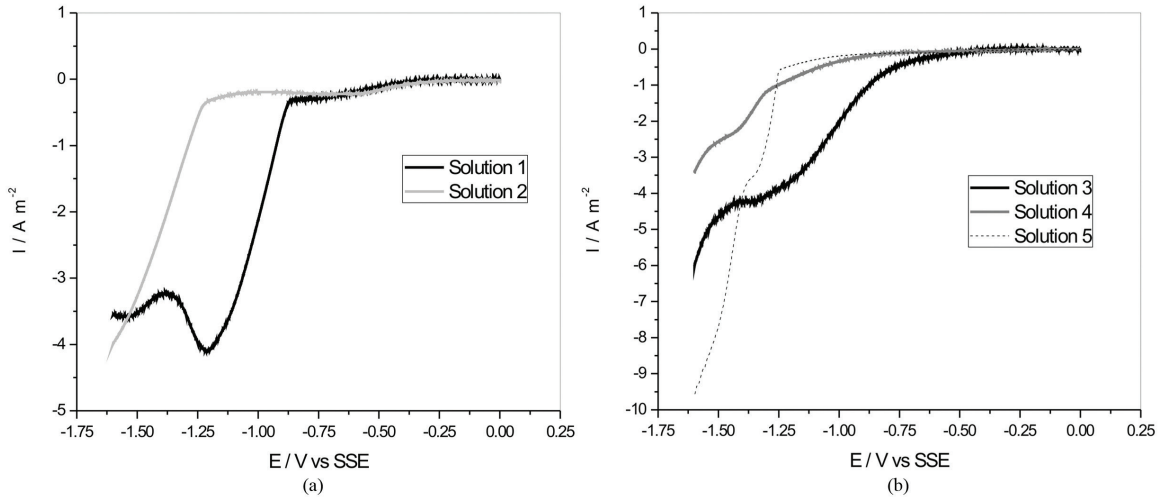

Figure 1. Cathodic scans of the solutions containing one of the ions (Co (II) or Zn (II)), without (a) or with (b) citrate. Figure 1b also shows the cathodic linear voltametric curve of the graphite substrate in solution 5 of Table 1.

shifted to more positive values when sodium citrate was added to the baths (Solutions 3 and 4), as shown in both Figure 1b and Table 3. This result may indicate that in the conditions of the present experiments, the reduction of Co-Citrate or Zn-Citrate complexes could be energetically more favorable than their respective aquo complexes. Similar to what has been observed for the metallic aquo complexes, the potentials for the reduction of Co-Citrate complexes are considerably more positive than those for the Zn-Citrate ones at the same conditions. This result was expected based on their respective stability constant values and suggests that if a bath containing both ions and the citrate ligand was used, the alloy deposition process would be a normal one and Co (II) ions would reduce preferentially.

Table 3 also shows that the cathodic peak potentials (E_{cp}) are at more negative values than the E_{sd} ones. Although the E_{sd} cannot be considered the E_{eq} of a M^{n+}/M reduction pair in a foreign substrate, it is possible to suppose that this difference can be related to the fact that E_{cp} may involve not only the thermodynamic equilibrium potential but also the potential required for the deposition of metals onto a foreign substrate[28]. The differences between E_{cp} and E_{sd} for the studied deposition processes are also presented in Table 3 and it is possible to observe that the total potential required for the electrodeposition of the metallic citrate complexes are more negative than that obtained for the metallic aquo complexes. The differences observed for each studied solution indicate that the steps involved in the electrocrystallization process of both zinc and cobalt ions on graphite surface require different energies depending on the coordination sphere of the ionic species. Therefore, based on the values shown in Table 3, although the reduction of the metallic ions from their citrate complexes started at more positive potential, the overall energies needed for deposit cobalt or zinc from a Co-Citrate or Zn-Citrate complexes are higher than those needed to produce these metallic layers from their respective aquo complexes.

Figure 1b also presents the cathodic linear voltametric curves of the graphite substrate in the solution 5 of Table 1, aiming to compare the isolated processes of metal reduction from a citrate complex with the reduction process when both metallic ions are in the same citrate bath. It is important to point out that the simultaneous discharge of different ions on the cathode is not a simple process, and it can be influenced by several factors, such as the substrate surface, the current density or potential applied, as well as the changes in the structure and activity of each metal cation in the double layer[29,30].

It is possible to observe that the E_{sd} value for the alloy reduction occurred at potentials more negative than those of zinc and cobalt reduction, separately. A small shift in the applied potential to more negative values caused a rapid increase in the current density and the alloy curve cross both cobalt and zinc curves. This result may indicate that, at the conditions of these experiments, the content of the metal in the coating and the kind of deposition process (normal or anomalous), would depend on the applied potential or current density, which is in agreement with the results of Roventi et al.[11] and Kirilova et al.[12].

Table 3. Voltametric parameters obtained from linear voltametric experiments of Co^{2+} or Zn^{2+} solutions, containing or not sodium citrate 0.10 mol L^{-1}, on graphite electrode.

Voltametric parameters*	Potential/V vs SSE	
	No citrate	With citrate
E_{sd} (Co)	–0.870	–0.652
E_{cp} (Co)	–1.211	–1.350
E_{cp} (Co) - E_{sd} (Co)	–0.341	–0.698
E_{sd} (Zn)	–1.215	–0.866
E_{cp} (Zn)	–1.584	–1.438
E_{cp} (Zn) - E_{sd} (Zn)	–0.369	–0.572

*E_{sd} – starting deposition potential; E_{cp} – cathodic peak potential.

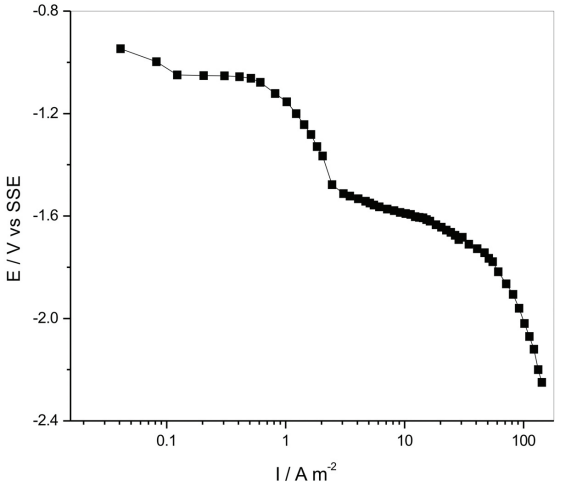

Figure 2. Cathodic galvanostatic polarization curves of the steel substrate in Bath 5 of Table 1.

Rashwan et al.[7] showed that, for the steel polarization in a Zn-Co electrolyte containing glycine 1 mol L^{-1}, the curve of the alloy lied between those of isolated metals, indicating that glycine electrolyte was able to brought the reduction potentials of the metallic ions together and the nobler metal (cobalt) deposited at less negative potentials, while the less noble metal (zinc) co-deposited at more negative potentials[7,31,32]. Therefore, normal co-deposition would take place, independent of the current density or potential applied. However, these authors have also shown that the expected behavior was not verified indeed when the alloys were produced and anomalous deposition was always observed. These results show the limitation of using only these experiments to verify the deposition process of metallic alloy coatings.

3.2. *Cathodic galvanostatic polarization curves*

Figure 2 presents the cathodic polarization curve of the steel substrate in Bath 5, earlier described in Table 1. The main goal of this experiment was to select the values of **I** to be used in the electrodeposition of the alloy, which were: 10 A m^{-2}, 20 A m^{-2}, 40 A m^{-2} and 80 A m^{-2}.

At smaller current densities, the zinc deposition in a Zn-Co alloy is generally preferential, as a result of the zinc

hydroxide oscillation[1,3]. Therefore, the increase in current density may favor the cobalt deposition. Similar results were shown by Karahan et al.[1] and Roventi et al.[11] in the deposition of Zn-Co alloys from a bath containing sodium citrate.

3.3. *Electrodeposition experiments*

As the aim of this work was to produce Co-rich coatings, six values of **I** were selected, based on from the polarization curve of Figure 2, to perform the electrodeposition of the Zn-Co alloy on steel substrate, from Bath 5 of Table 1. However, the coatings electrodeposited at **I** values smaller than 10 A m^{-2} were not adherent to the steel substrate. Therefore, only four values of **I** (10 A m^{-2}, 20 A m^{-2}, 40 A m^{-2} and 80 A m^{-2}) were considered in this work. The colors of the produced coatings varied from light to dark gray and from opaque to bright, as a function of **I**.

The $\mathbf{E}_f$ values were always low, ranging from 23 + 3 to 42 + 1 %. The maximum $\mathbf{E}_f$ value was obtained for **I** = 40 A m^{-2}, as shown in Figure 3. Since $\mathbf{E}_f$ is related to the content of metals deposited, these results indicated that other parallel reactions might have been competing with the main reactions (the metallic ions reduction), decreasing the values of $\mathbf{E}_f$. The most probable parallel reaction is the hydrogen evolution reaction (HER), which may have consumed part of the applied **I** causing the low $\mathbf{E}_f$ values.

Figure 4 presents the results obtained for **% m/m Zn** and **% m/m Co**, for each value of **I** studied. The **% m/m Co** in solution was also calculated (47.43 % m/m) and it was considered as the base value of **% m/m Co**[5]. It can be noted that, except for **I** = 10 A m^{-2}, normal deposition processes occurred in the experiments performed with Bath 5. Most of the values of **% m/m Co** are always higher than that of the base value of **% m/m Co**, and also higher than those of **% m/m Zn**, showing that the deposition of the nobler metal was favored in the studied conditions and that Co-rich coatings were produced. There was also a significant trend ($p<0.05$) of increasing **% m/m Co** and decreasing **% m/m Zn** with **I**. Therefore, the deposition of cobalt was enhanced by this parameter.

Both Gharahcheshmeh and Sohi[8] and Kirilova et al.[12] have reported the dependence of **% m/m Co** on **I**, even though none of these authors have obtained normal deposition. In fact, it is usually found in the literature reports concerning the anomalous nature of Zn-Co alloy electrodeposition process, both in the absence and in the presence of complexant agents and/or additives[2,6,7,33,34]. It is important to note, however, that most of these works used $\mathbf{[Co^{2+}] < [Zn^{2+}]}$, while in the present study it was used a solution where $\mathbf{[Co^{2+}] = [Zn^{2+}]}$. Both Gómez and Vallés[6] and Cao[35] have shown that the Zn-Co deposition process was also dependent on the $\mathbf{[Co^{2+}]}$. Even though, these authors affirmed that cobalt deposition was still greatly inhibited and anomalous deposition occurs when $\mathbf{[Co^{2+}] = [Zn^{2+}]}$.

The presence of a complexant agent may also interfere on the alloy deposition process if one of the ions in solution is more intensively complexed than the other. Citrate is a tri-carboxylate anion and it usually forms stable metallic complexes, which are shifted to smaller wavelength length, when analyzed by spectrophotometry[36]. Since the stability

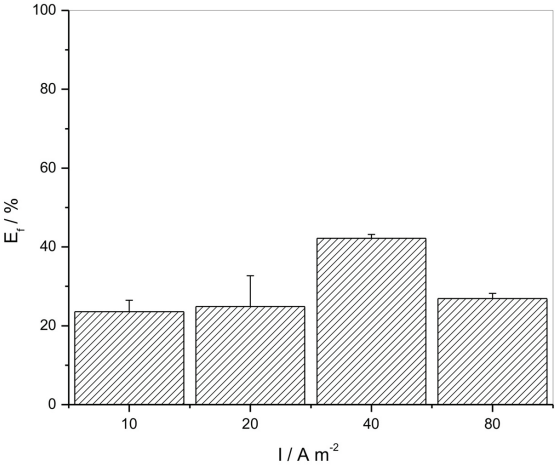

Figure 3. Average values of cathodic efficiency ($\mathbf{E}_f$) of the deposited alloy on steel substrate.

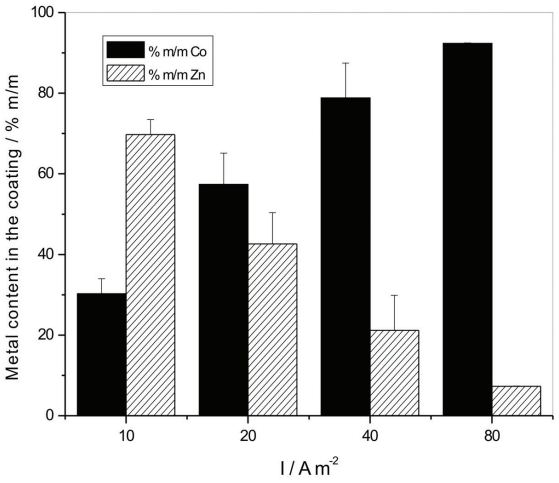

Figure 4. Average values of zinc and cobalt contents in the coatings (**% m/m Zn** and **% m/m Co**) produced at different values of **I**.

constant for Zn-Citrate complex is almost three orders of magnitude higher than that for the Co-citrate complex[27], it is expected that most of the Zn (II) ions were preferentially as Zn-citrate complexes in the solution, while most of the Co (II) ions could be reduced directly from the aquo complexes. Similar results were found for Survila et al.[37] for Sn-Co alloys in citrate baths at similar conditions.

Szczygieł et al.[2], have also studied sodium citrate as a complexant agent for Zn-Co alloy deposition in a bath using the same metallic ion relationship as it was used in the present research ($\mathbf{[Co^{2+}] = [Zn^{2+}]}$). Nonetheless, they observed anomalous deposition for Zn-Co alloys at high **I** values. It is important to point out that, differently from our work in which $\mathbf{[Cit^{3-}] = 2\,[Zn^{2+}]}$, the amount of ligand used by these authors ($\mathbf{[Zn^{2+}] = [Cit^{3-}]}$) was probably insufficient to complex all Zn (II) ions in the solution.

Even though the complexant concentration in Bath 5 was enough to complex all the Zn (II), the condition **I** = 10 A m^{-2} still stimulated zinc deposition. Therefore, it

is important to point out that both the presence of a ligand and its concentration, as well as the **I** value used must be considered when studying the conditions to obtain normal or anomalous Zn-Co deposition process, or even Co-rich coatings.

At pH value of solution 5 (Table 1), the hydrogen evolution reaction (HER) is the main parallel reaction in the process. Since H^+ ions from water were reduced, the interface metal/solution was enriched of OH^-, which could have enhanced the zinc deposition as hydroxide, originating the zinc hydroxide oscillation process and, consequently, the observed anomalous deposition. Even though this kind of deposition process was observed at 10 A m^{-2}, the coatings were Co-rich ones, presenting approximately 30 % m/m Co. Therefore, another highlight that could explain the high amount of Co obtained, even at 10 A m^{-2}, and the normal deposition process in Zn-Co citrate baths at higher **I** values would be the buffering effect of citrate that could have contributed to decrease the formation of zinc hydroxide, which is considered the responsible for the oscillatory zinc hydroxide process[8]. It means that the zinc deposition was hindered, while cobalt deposition was enhanced in the presence of citrate. Similar results were obtained by Trejo et al.[18] using benzidilacetone in the bath. However, new experiments concerning the local pH measurements on the electrode/solution interface are still needed to reach a final conclusion about this topic.

Using $\mathbf{E}_f$ and the contents of the elements in the alloy (**% m/m Co** and **% m/m Zn**) data, it was possible to calculate the partial current densities of each one of the metals ($\mathbf{I}_{Zn}$, $\mathbf{I}_{Co}$) and of the HER process ($\mathbf{I}_H$). It is possible to observe, in Figure 5, that the transition from anomalous to normal deposition occurred with the increasing **I**, as earlier seen in Figure 4. Moreover, a strong decrease for the $\mathbf{I}_{Zn}$ curve can be observed at high values of **I**. These results confirm that the increase in **I** promoted the deposition of cobalt in the alloy.

It is interesting to note that, comparing to the $\mathbf{I}_{Zn}$ and $\mathbf{I}_{Co}$ curves, the $\mathbf{I}_H$ curve is always the closest one to the total **I** curve. This result justifies the low values of $\mathbf{E}_f$ presented in Figure 3, and it means that most of applied **I** was used by the HER process. Even though, it is important to remember that both metals could have also be deposited as hydroxides under these conditions, and that the $\mathbf{I}_H$ curve was obtained by the difference between the values of $\mathbf{I}_{Zn}$ and $\mathbf{I}_{Co}$ and may not be entirely conclusive.

3.4. *Characterization of selected coatings*

Based on the results obtained for the metal contents (**% m/m Co** and **% m/m Zn**) the coatings produced from experiments 1 (30.25 % m/m Co and 69.75 % % m/m Zn) and 4 (92.38 % m/m Co and 7.32 % m/m Zn) of Table 2, were selected to be electrochemically, morphologically, and microstructurally characterized. These experiments represent conditions in which Co-rich coatings containing **% m/m Co < % m/m Zn** and **% m/m Co > % m/m Zn**, respectively, were produced. The distribution of the elements in the coatings is shown by the EDS analysis (Figure 6) and corroborates the results previously presented in Figure 4.

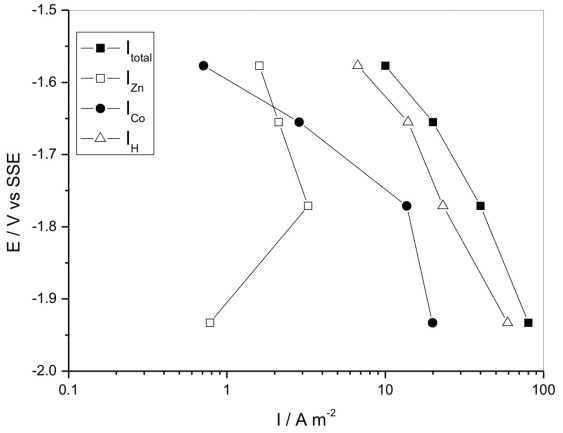

Figure 5. Partial current densities of each one of the deposited metals ($\mathbf{I}_{Zn}$, $\mathbf{I}_{Co}$) and of the HER process ($\mathbf{I}_H$).

3.4.1. Morphological and microstructural evaluation

Figure 7 shows the surface morphology of the Zn-Co coatings produced from the experiments 1 and 4 (Table 2). From the $\mathbf{E}_f$ results, it is possible to suppose that thin coatings were produced for both **I** values studied. Comparing the surface morphologies of the coatings obtained from experiments 1 (Figure 7a) and 4 (Figure 7b), it can be noted that an increase in **I**, and consequently, in **% m/m Co** as shown in Figure 4, resulted in a decrease of the grain size. At lower **I** values, heterogeneous surfaces with several clumps and irregular grains were obtained, while fine grains and higher surface homogeneity was observed from the samples produced from experiment 4. Similar results have been found in literature for Zn-Co and Zn-Ni coatings[9,38]. These results show that the variable **I** actually interfered in both the composition and the morphology of the deposited layers.

The diffractograms of the coatings produced under the selected conditions (Figure 8a) presented relatively sharp diffraction lines. However, an amplification of the diffratograms (Figure 8b) show broad and low intensity peaks, which can be explained by the low thickness of the coatings and the small particle diameters (26 nm and 22 nm, for experiments 1 and 4, respectively). In fact, several authors have showed that XRD analysis is not always able to identify the deposited Zn–Co or Zn-Ni alloys phases because of the presence of a large amount of crystallites too small to be resolved by this technique[9,14,38-40].

It is important to point out that most of the electrolytically obtained alloys, produced from different baths, usually consist of fine crystals, non-uniform in composition and characterized by a considerable distortion of the crystal lattice, originated during the formation of the non-equilibrium phases at the cathode, which occurs at high overpotential values. As a result, it is normally difficult to analyze these alloy deposits by X-rays examination and, in some cases, phases present in a given deposit can be only partially revealed[29,39]. In the present work, the coatings were obtained at high current density values and, consequently, at high overpotentials. Therefore, it is possible to relate any lattice distortion to the production of non-equilibrium phases.

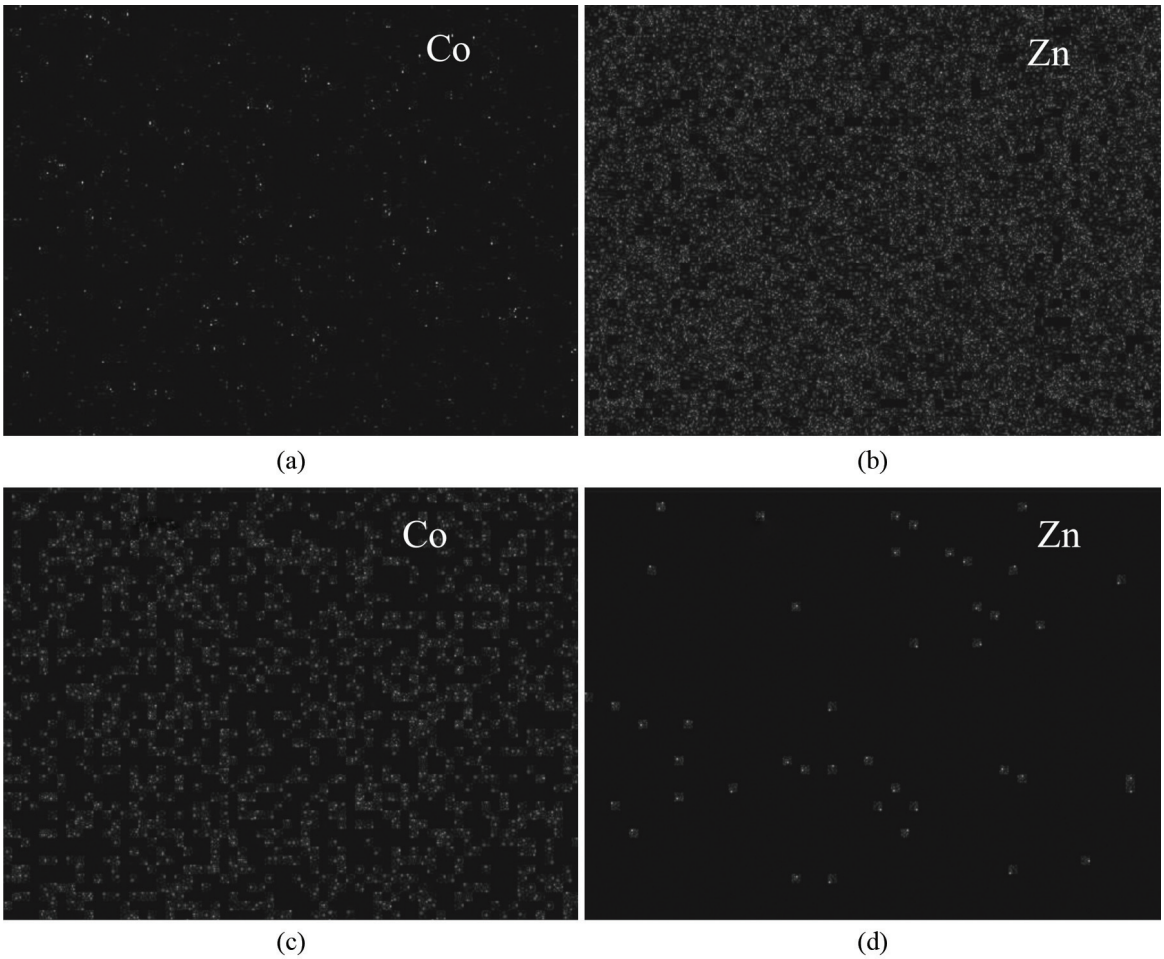

Figure 6. EDS analysis showing the distribution of the elements in the coatings selected from Table 2. Experiment 1: (a) Co and (b) Zn; Experiment 4: (c) Co and (d) Zn.

Lattice distortion can be responsible for non-homogeneous microscopic residual stress and can significantly contribute to the coating microhardness. Moreover, all coatings were produced at room temperature and the thermal mismatch could also contribute to macroscopic residual stress as well as to the microhardness values of the electrodeposited layers[39-41]. In some cases, non cataloged crystalline phases were obtained[9,14,41].

Table 4 presents the experimental values obtained for 2θ and *d* of the main lines observed for both experiments. Since some phases observed in the electrodeposited Zn–Co alloys were not identified by the available XRD pattern databases[42], it was also used the literature references[10,43,44] to identify the experimental lines obtained from both experiments.

There most difference between the diffractograms of the coatings produced from experiments 1 and 4 is the intensity of the diffraction lines. The low intensities observed for experiment 4 agrees with the small grain size verified for this experiment (Figure 7b). The more intense diffraction lines (Figure 8a) are seen in the coating produced from experiment 1 and are correspondent with the Fe (110) line at 2θ = 44.60° (datasheet no. 06-0696) and the γ-$Zn_{21}Co_5$ (330) line at 2θ = 43.14°[10,43]. Small diffraction lines, corresponding to Zn phases (datasheet no. 04-0831) were also verified. The γ-$Zn_{21}Co_5$ (330) line was smaller and broader in the experiment 4, confirming that a coating with **% m/m Co >> % m/m Zn** and small grains was produced.

The presence of γ-$Zn_{21}Co_5$ was reported in coatings produced at high current densities, when the deposition potential becomes more negative[3]. Rashwan et al.[7] observed that, at lower current densities, the coating consisted of a cubic structure of γ-$Zn_{21}Co_5$, while in higher values of current density, the coating were composed of both a cubic phase of γ-$Zn_{21}Co_5$ and another phase γ_2-$Zn_{13}Co$ with monoclinic structure. Deposits with **% m/m Co** above 3 % m/m show a diffraction peak that is associated with the formation of the γ- phases[45]. In addition, these phases have been earlier observed in Co-rich coatings containing from 10 % m/m to 15 %m/m[10,43,46]. In the present work, the γ_2-$Zn_{13}Co$ phase was not verified. These results indicate that deposition conditions that enhance cobalt deposition may produce γ-ZnCo phases phases

However, this γ-phase diffraction line was significantly decreased in the coating containing almost 92 % m/m Co. A magnification of the diffractograms presented in Figure 8a ranging from 2θ = 40° to 2θ = 47° (Figure 8b), shows

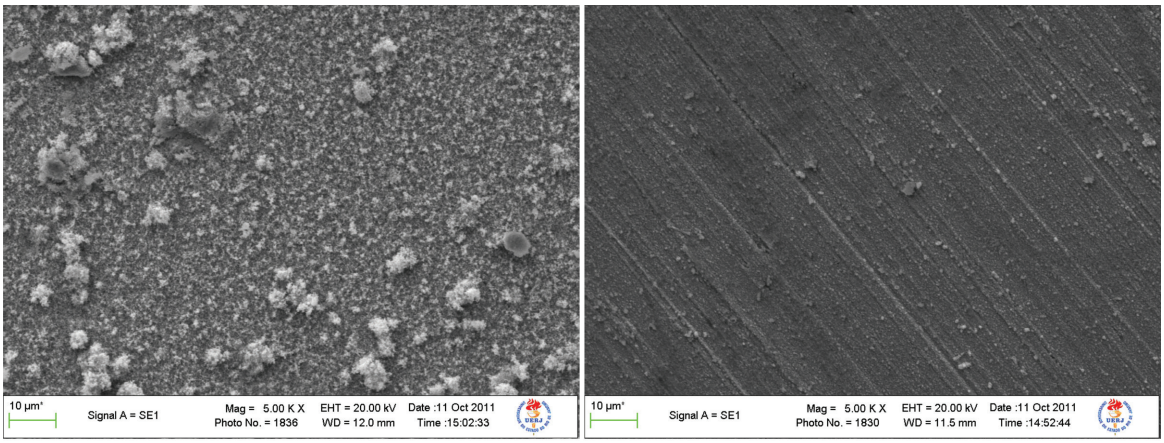

(a) (b)

Figure 7. Surface morphology evaluation of the Zn-Co coatings produced from the selected experiments shown in Table 2. (a) Experiment 1; (b) Experiment 4.

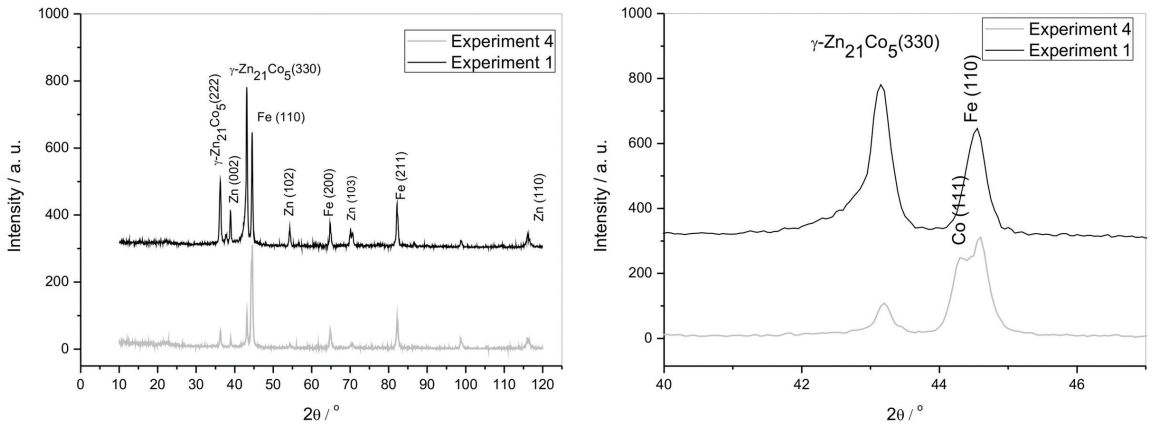

(a) (b)

Figure 8. (a) XRD analysis of the coatings produced from experiments 1 and 4 (Table 2); (b) Magnification of Figure (a).

Table 4. *d* (*h k l*) values for the Zn-Co coatings produced from the selected experiments of Table 2.

Observed 2θ	Observed *d* (*h k l*)	*d* (*h k l*) carbon steel AISI 1020	*d* (*h k l*) γ-ZnCo (cubic)	*d* (*h k l*) Co	*d* (*h k l*) Zn
36.30	2.471		2.470		2.473
38.97	2.310				2.308
43.20	2.092		2.090		2.091
44.32	2.041			2.047	
44.60	2.029	2.027			
54.36	1.687				1.687
64.86	1.436	1.433			
70.50	1.336				1.330
82.25	1.172	1.170			1.173
98.85	1.014			1.015	
116.22	0.907				0.906

Table 5. Results of $\mathbf{I}_{corr}$, $\mathbf{E}_{corr}$, **C.R.**, and $\mathbf{R}_p$ of the selected carbon steel/alloy coating systems in a 0.5 mol L^{-1} NaCl solution.

Experiment no.	I_{corr}/μA cm^{-2}	C. R./mm $year^{-1}$	E_{corr}/V_{SCE}
1	2.4	4.9 x 10^{-2}	–0.974
4	7.0	1.4 x 10^{-1}	–1.119

a shoulder at 2θ = 44.20°, in the broad Fe (110) line in experiment 4 (**% m/m Co > % m/m Zn**), which corresponds to Co (111) line (datasheet no. 15-0806). This result suggests that a Co segregated phase was preferable obtained under the conditions of experiment 4.

3.4.2. Corrosion experiments

The $\mathbf{I}_{corr}$, corrosion rate (**C.R.**), and $\mathbf{E}_{corr}$ of the selected carbon steel/alloy coating systems in a 0.5 mol L^{-1} NaCl solution are presented in Table 5. It is possible to observe that there are significant differences among the coatings produced from experiments 1 and 4. The $\mathbf{E}_{corr}$ of the coating produced in experiment 4 was shifted to more negative values, when compared to that produced at the conditions of experiment 1 (**% m/m Co < % m/m Zn**). It was expected that the increase in the Co codeposition in a Zn-Co alloy changes the coating protection process from a sacrificial coating to a protective one[3]. However, the $\mathbf{E}_{corr}$ values of both studied coating/substrate systems were more negative than that of naked steel in the same medium (–0.583 V_{SCE}), showing that all the coatings produced behave as sacrificial coating. It could be explained by the small thickness of the coatings and for the Zn-rich phases observed by XRD analysis, due to the segregation of the excess of cobalt.

Table 5 also shows that the smallest values of $\mathbf{I}_{corr}$ and **C.R.** were obtained for the coatings where **% m/m Co < % m/m Zn** (experiment 1). It is known that the presence of cobalt in the Zn-Co coating increases the dissolution of zinc in a solution of NaCl, causing the reaction of the metal ion with Cl^- to form zinc hydroxide chloride (ZHC) according to the following reaction[8], ensuring higher protection ability for the Zn-Co coatings:

$$5Zn^{2+} + 8OH^- + 2Cl^- + H_2O \rightarrow Zn_5(OH)_8Cl_2.H_2O$$

Lichušina et al.[10] have shown that the increase in **% m/m Co** (15 – 18 % m/m Co) produced Zn-Co alloy coatings with a corrosion resistance about threefold higher than the coatings with low cobalt content (1-3 % m/m Co). Bajat et al.[47] have found the smallest $\mathbf{I}_{corr}$ (4.0 μA cm^{-2}) for a coating containing approximately 18 % m/m Co, which is comparable to the results obtained for the coating containing ~ 30 % m/m Co (2.4 μA cm^{-2}, experiment 1). In addition, it is known that the γ - $Zn_{21}Co_5$ alloy phase is characteristic of a high corrosion resistance coating and the absence of additional phases is favorable to the alloy stability[46]. In the present work, although both coatings presented the γ - $Zn_{21}Co_5$, the presence of a segregated Co-phase and the low thickness of the coatings may have contributed to the worse performance of the coating produced from experiment 4.

4. Conclusions

Both **I** and the presence of sodium citrate as a ligand influenced on the process of deposition of the alloy, affording adherent Zn-Co alloy coatings with different chemical compositions. The $\mathbf{E}_f$ values were low in all cases. The $\mathbf{I}_H$ values corroborated these findings by showing that the reduction reaction of H^+ was always priority over the deposition of metals. In addition, the action of citrate as a ligand may have caused an increase in the total energy to reduce both metallic ions.

I influenced the deposition process and affected significantly ($p<0.05$) the composition of the alloy. Low values of **I** stimulated anomalous deposition and the production of coatings with higher **% m/m Zn** while an increase of **I** promoted a normal type deposition and coatings with higher **% m/m Co**.

Although the coatings containing **% m/m Co > % m/m Zn** showed a homogeneous morphology with the smallest grain size, the best anticorrosive performance was obtained by the coating containing approximately 30 **% m/m Co**. It means that, beside the morphological characteristics, the presence of the γ - $Zn_{21}Co_5$ alloy phase and no segregated phases must have contributed to the performance of the coating produced from experiment 1.

Acknowledgments

The authors would like to thank the Rio de Janeiro Research Foundation (FAPERJ), the Brazilian National Research Council (CNPq), the State University of Rio de Janeiro (UERJ), and the Prociência Program for financial support. We would like also to thank Antônio Vitor de Castro Braga for technical support, M.Sc. Márcio Franklin de Oliveira for the SEM analysis, and Professor Deborah Vargas for helping in the X-rays analysis.

References

1. Karahan IH, Karabulut O and Alver UA. Study on electrodeposited Zn-Co alloys. *Physica Scripta*. 2009; 79(5):1-6.
2. Szczygiel B, Laszczynska A and Tylus W. Influence of molybdenum on properties of Zn-Ni and Zn-Co alloy coatings. *Surface and Coatings Technology*. 2010; 204(9-10):1438-1444. http://dx.doi.org/10.1016/j.surfcoat.2009.09.042
3. Chen PY and Sun IW. Electrodeposition of cobalt and zinc-cobalt alloys from a lewis acidic zinc chloride-1-ethyl-3-methylimidazolium chloride molten salt. *Electrochimica Acta*. 2001; 46(8):1169-1177. http://dx.doi.org/10.1016/S0013-4686(00)00703-9
4. Lodhi ZF, Mol JMC, Hovestad H, Terryn H and Wit JHW. Electrodeposition of Zn-Co and Zn-Co-Fe alloys from acid chloride electrolytes. *Surface and Coatings Technology*. 2007; 202(1):84-90 http://dx.doi.org/10.1016/j.surfcoat.2007.04.070
5. Brenner A. *Electrodeposition of alloys*. New York: Academic Press; 1963. Volume 2.
6. Gómez E and Vallés E. Electrodeposition of zinc + cobalt alloys: initiations and development of anomalous co-deposition. *Journal of Electroanalytical Chemistry*. 1997; 421(1-2):157-163. http://dx.doi.org/10.1016/S0022-0728(96)04835-8
7. Rashwan SM, Mohamed AE, Abdel-Wahaab SM and Kamel MM. Electrodeposition and characterization of thin layers of Zn-Co alloys obtained from glycinate baths. *Journal of Applied Electrochemistry*. 2003; 33(11):1035-1042. http://dx.doi.org/10.1023/A:1026280109296
8. Gharahcheshmeh MH and Sohi MH. Study of the corrosion behavior of zinc and Zn-Co alloy electrodeposits obtained from alkaline bath using direct current. *Materials Chemistry and Physics*. 2009; 117(2-3):414-421. http://dx.doi.org/10.1016/j.matchemphys.2009.06.009
9. Lodhi ZF, Tichelaar FD, Kwakernaak C, Mol JMC, Terryn H and Wit JHW. A combined composition and morphology study of electrodeposited Zn-Co and Zn-Co-Fe alloy coatings. *Surface and Coatings Technology*. 2008; 202(12):2755-2764. http://dx.doi.org/10.1016/j.surfcoat.2007.10.017
10. Lichušina S, Sudavičius A, Juškėnas R and Bučinskienė D. Deposition of cobalt rich Zn-Co alloy coatings of high corrosion resistance. *Transactions of the Institute of Metal Finishing*. 2008; 86(3):141-147. http://dx.doi.org/10.1179/174591908X304162
11. Roventi G, Bellezze T and Fratesi R. Electrochemical study on the inhibitory effect of the underpotential deposition of Zn-Co alloy electrodeposition. *Electrochimica Acta*. 2006; 51(13): 2691-2697. http://dx.doi.org/10.1016/j.electacta.2005.08.002
12. Kirilova I, Ivanov I and Rashkov ST. Electrodeposition of Zn-Co alloy coatings from sulfate–chloride electrolytes. *Journal Applied Electrochemistry*. 1997; 27(12):1380-1384. http://dx.doi.org/10.1023/A:1018425129532
13. Lima P No, Correia AN, Colares RP and Araujo WS. Corrosion study of electrodeposited Zn and Zn-Co coatings in chloride medium. *Journal of Brazilian Chemical Society*. 2007; 18(6);1164-1175. http://dx.doi.org/10.1590/S0103-50532007000600010
14. Gharahcheshmeh MH and Sohi MH. Electrochemical studies of zinc-cobalt alloy coatings deposited from alkaline baths containing glycine as complexing agent. *Journal of Applied Electrochemistry*. 2010; 40(8):1563-1570. http://dx.doi.org/10.1007/s10800-010-0142-6
15. Mac Kinnon DJ and Brannendaqui JM. Evaluation of organic additives as levelling agents for zinc electrowinning from chloride electrolytes. *Journal Applied Electrochemistry*. 1982; 12(1):21-31. http://dx.doi.org/10.1007/BF01112061
16. Ballesteros JC, Díaz-Arista P, Meas Y, Ortega R and Trejo G. Zinc electrodeposition in the presence of polyethylene glycol 20000. *Electrochimica Acta*. 2007; 52(1):3686-3696. http://dx.doi.org/10.1016/j.electacta.2006.10.042
17. Michailova E, Peykova M, Stoychev D and Milchev A. On the role of surface active agents in the nucleation step of metal electrodeposition on a foreign substrate. *Journal of Electroanalytical Chemistry*. 1994; 366(1-2):195-202. http://dx.doi.org/10.1016/0022-0728(93)03228-H
18. Trejo G, Ortega R, Meas Y, Chainet E and Ozil P. Effect of benzylideneacetone on the electrodeposition mechanism of Zn-Co alloy. *Journal of Applied Electrochemistry*. 2003; 33(5):373-379. http://dx.doi.org/10.1023/A:1024466604939
19. Vagramyan TA and Solov'eva ZA. Technology of electrodeposition. Teddington: Robert Drapper; 1961.
20. Fujiwara Y and Enomoto H. Electrodeposition of β′-Brass from cyanide baths with accumulative underpotential deposition of zn articles. *Journal of The Electrochemical Society*. 2000; 147(5):1840-1846. http://dx.doi.org/10.1149/1.1393444
21. Hosseini MG, Ashassi-Sorkhabi H and Ghiasvand HAY. Electrochemical studies of Zn-Ni alloy coatings from non-cyanide alkaline bath containing tartrate as complexing agent. *Surface and Coatings Technology*. 2008; 202(13):2897-2904. http://dx.doi.org/10.1016/j.surfcoat.2007.10.022
22. Lan CJ, Liu WY, Ke ST and Chin TS. Potassium salt based alkaline bath for deposition of Zn-Fe alloy. *Surface and Coatings Technology*. 2006; 201(6):3103-3108. http://dx.doi.org/10.1016/j.surfcoat.2006.06.027
23. Karahan IH and Çetinkara HA. Study of effect of boric acid on Zn-Co alloy electrodeposition from acid baths and on composition, morphology and structure of deposit. *Transactions of the Institute of Metal Finishing*. 2011; 89(2):99-103. http://dx.doi.org/10.1179/174591911X12968393517774
24. Hegde AC and Thangaraj V. Electrodeposition and characterization Zn-Co alloy. *Russian Journal of Electrochemistry*. 2009; 45(7):756-761. http://dx.doi.org/10.1134/S1023193509070076
25. Ferreira FBA, Silva FLG, Luna AS, Lago DCB and Senna LF. Response surface modeling and optimization to study the influence of deposition parameters on the electrodeposition of Cu-Zn alloys in citrate médium. *Journal of Applied Electrochemistry*. 2007; 37(4):473-481. http://dx.doi.org/10.1007/s10800-006-9278-9
26. Silva FLG, Cruz VGM, Garcia JR, Luna AS, Lago DCB and Senna LF. Response surface analysis to evaluate the influence of deposition parameters on the electrodeposition of Cu-Co alloys in citrate médium. *Journal of Applied Electrochemistry*. 2008; 38(12):1763-1769. http://dx.doi.org/10.1007/s10800-008-9630-3
27. Lurie JU. *Handbook of analytical chemistry*. Moscow: Mir Publishers, 1978.
28. Palomar-Pardavé M, González I, Soto AB and Arce EM. Influence of the coordination sphere on the mechanism of cobalt nucleation onto glassy carbon. *Journal of Electroanalytical Chemistry*. 1998; 443(1):125-136. http://dx.doi.org/10.1016/S0022-0728(97)00496-8
29. Vagramyan TA. Electrodeposition of alloys; mechanism of simultaneous reaction of metal ions. In: Kruglikov SS, editor.

Electrochemistry. Jerusalem: Israel Program of Scientific Translation; 1970.

30. Lainer VI. *Modern electroplating*. Jerusalem: Israel Program of Scientific Translation; 1970.
31. Senna LF, Díaz SL and Sathler L. Electrodeposition of copper-zinc alloys in pyrophosphate-based electrolytes. *Journal of Applied Electrochemistry*. 2003; 33(12):1155-1161. http://dx.doi.org/10.1023/B:JACH.0000003756.11862.6e
32. Farias LT, Luna AS, Lago DCB and Senna LF. Influence of cathodic current density and mechanical stirring on the electrodeposition of Cu-Co alloys in citrate bath. *Materials Research*. 2008; 11(1):1-9. http://dx.doi.org/10.1590/S1516-14392008000100002
33. Ortiz-Aparicio JL, Meas Y, Trejo G, Ortega R, Chapman TW, Chainet E et al. Electrodeposition of zinc-cobalt alloy from a complexing alkaline glycinate bath. *Electrochimica Acta*. 2007; 52(14): 4742-4751. http://dx.doi.org/10.1016/j.electacta.2007.01.010
34. Prasad KA, Giridhar P, Ravindran V and Muralidharan VS. Zinc-cobalt alloy: electrodeposition and characterization. *Journal of Solid State Electrochemistry*. 2001; 6(1):63-68. http://dx.doi.org/10.1007/s100080000160
35. Cao Y. *Cobalt electrocrystallization and codeposition with zinc*. [Thesis]. Columbia: University of Missouri; 2000.
36. Watanabe RH. *Aplicação de complexos de metais de transição coordenados a típicos aditivos orgânicos de banhos eletrolíticos em eletrodeposição binária de metais*. [Tese]. São Carlos: Universidade de São Paulo; 2008.
37. Survila A, Mockus Z and Kanapeckaitė S. Kinetics of Sn and Co codeposition in citrate solutions. *Electrochimica Acta*. 2000; 46(4):571-577. http://dx.doi.org/10.1016/S0013-4686(00)00633-2
38. Alfantazi AM, EI-Sherik AM and Erb U. The role of nickel in the morphology evolution of pulse plated Zn-Ni alloy coatings. *Scripta Metallurgica et Materialia*. 1994; 30(10):1245-1250. http://dx.doi.org/10.1016/0956-716X(94)90253-4
39. Senna LF, Díaz, SL and Sathler L. Hardness analysis and morphological characterization of copper-zinc alloys produced in pyrophosphate-based electrolytes. *Materials Research*. 2005; 8(3):275-279. http://dx.doi.org/10.1590/S1516-14392005000300009
40. Garcia JR, Lago DCB, Silva FLG, D'Elia E, Luna AS and Senna LF. Statistic evaluation of cysteine and allyl alcohol as additives for Cu-Zn coatings from citrate baths. *Materials Research*. 2013; 16(2):392-403. http://dx.doi.org/10.1590/S1516-14392012005000181
41. Senna LF, Achete CA, Mattos OR and Hirsch T. Characterization of PVD TiCN layers by physical and electrochemical methods. *Surface Engineering*. 2005; 21(2):144-150. http://dx.doi.org/10.1179/174329405X40876
42. Joint Committee on Powder Diffraction Standards - JCPDS. *Powder Diffraction File*. Pennsylvania: ICDD; 2000. CD-ROM.
43. Gómez E, Alcobe X and Vallés E. Characterisation of zinc+cobalt alloy phases obtained by electrodeposition. *Journal of Electroanalytical Chemistry*. 2001; 505(1-2):54-61. http://dx.doi.org/10.1016/S0022-0728(01)00450-8
44. Eliaz N, Venkatakrishna K and Hegde AC. Electroplating and characterization of Zn-Ni, Zn-Co and Zn-Ni-Co alloys. *Surface and Coatings Technology*. 2010; 205(7):1969-1978. http://dx.doi.org/10.1016/j.surfcoat.2010.08.077
45. Shukla, RK and Srivastava SC. Studies of electrodeposition of Ni-Co-Zn alloys. *Surface and Coatings Technology*. 1984; 21(1):11-17. http://dx.doi.org/10.1016/0376-4583(84)90143-2
46. Lichušina S, Chodosovskaja A, Sudavičius A, Juškėnas R, Bučinskienė D, Selskis A et al. Cobalt-rich Zn-Co alloys: electrochemical deposition, structure and corrosion resistance. *Chemija*. 2008; 19(1):25-31.
47. Bajat JB, Stanković S, Jokić BM and Stevanović SI. Corrosion stability of Zn-Co alloys deposited from baths with high and low Co content: sthe influence of deposition current density. *Surface and Coatings Technology*. 2010; 204(16-17):2745-2753. http://dx.doi.org/10.1016/j.surfcoat.2010.02.032